



A density functional theory study on structures, stabilities, and electronic and magnetic properties of Au_nC ($n = 1-9$) clusters



Xiao-Fei Hou^a, Li-Li Yan^a, Teng Huang^a, Yu Hong^a, Shou-Kui Miao^a, Xiu-Qiu Peng^b, Yi-Rong Liu^{a,*}, Wei Huang^{a,b,*}

^aLaboratory of Atmospheric Physico-Chemistry, Anhui Institute of Optics & Fine Mechanics, Chinese Academy of Sciences, Hefei, Anhui 230031, China

^bSchool of Environmental Science & Optoelectronic Technology, University of Science and Technology of China, Hefei, Anhui 230026, China

ARTICLE INFO

Article history:

Received 16 November 2015

In final form 14 March 2016

Available online 23 March 2016

Keywords:

Gold cluster

Carbon

Basin-Hopping

Density functional theory

ABSTRACT

The equilibrium geometric structures, relative stabilities, electronic stabilities, and electronic and magnetic properties of the Au_nC and Au_{n+1} ($n = 1-9$) clusters are systematically investigated using density functional theory (DFT) with hyper-generalized gradient approximation (GGA). The optimized geometries show that one Au atom added to the Au_{n-1}C cluster is the dominant growth pattern for the Au_nC clusters. In contrast to the pure gold clusters, the Au_nC clusters are most stable in a quasi-planar or three-dimensional (3D) structure because the C dopant induces the local non-planarity, with exceptions of the $\text{Au}_{6,8}\text{C}$ clusters who have 2D structures. The analysis of the relative and electronic stabilities reveals that the Au_4C and Au_6 clusters are the most stable in the series of studied clusters, respectively. In addition, a natural bond orbital (NBO) analysis shows that the charges in the Au_nC clusters transfer from the Au_n host to the C atom. Moreover, the Au and C atoms interact with each other mostly via covalent bond rather than ionic bond, which can be confirmed through the average ionic character of the Au–C bond. Meanwhile, the charges mainly transfer between 2s and 2p orbitals within the C atom, and among 5d, 6s, and 6p orbitals within the Au atom for the Au_nC clusters. As for the magnetic properties of the Au_nC clusters, the total magnetic moments are $1 \mu_B$ for $n = \text{odd}$ clusters, with the total magnetic moments mainly locating on the C atoms for $\text{Au}_{1,3,9}\text{C}$ and on the Au_n host for $\text{Au}_{5,7}\text{C}$ clusters. However, the total magnetic moments of the Au_nC clusters are zero for $n = \text{even}$ clusters. Simultaneously, the magnetic moments mainly locate on the 2p orbital within the C atom and on the 5d, 6s orbitals within the Au atom.

© 2016 Elsevier B.V. All rights reserved.

1. Introduction

Atom clusters, as a new phase of matter, intermediate in size between separate atoms and bulk materials, and thus possess unique physical and chemical properties. One of the most extraordinary examples is the gold clusters, which play a central role in molecular electronic devices, catalysis, probe for biological diagnostics, etc. [1–18], while the bulk gold is normally ignored because of its chemical inertness. In addition, the electronic properties of atom clusters highly depend on their composition, size, shape, and valence state. All these parameters can be controlled and manipulated by doping a pure cluster M_n with one or more guest atoms X. It is specially effective when the M–X interactions

* Corresponding authors at: Laboratory of Atmospheric Physico-Chemistry, Anhui Institute of Optics & Fine Mechanics, Chinese Academy of Sciences, Hefei, Anhui 230031, China (W. Huang).

E-mail addresses: liuyirong@aiofm.ac.cn (Y.-R. Liu), huangwei6@ustc.edu.cn (W. Huang).

are stronger than the M–M ones, since under this circumstances, the structures of the M_n host will be changed a lot [19–26]. Due to the significant role in catalysis and nanotechnology, the gold clusters have been and continued to become an increasingly interesting topic of research from both fundamental and practical viewpoints. So far there have been a large amount of experimental and theoretical studies on the pure gold clusters with impurity atom X [27–37], and the most common are the transition metal impurities. In addition, as for the number of the dopant atoms, the single-doped situation predominates compared to the double-doped even triple-doped situation. All the cases mentioned above have been simply introduced in our previous investigation [38].

As for the situation of the C atom as the dopant, in summary, there are only a few studies. Pal et al. proved that all the lowest-energy structures of XAu_4 ($X = \text{C}, \text{Si}, \text{Ge}, \text{and Sn}$) clusters are the tetrahedron configuration [19]. Subsequently, a density functional theory (DFT) study shows that the lowest-energy structures of $\text{Au}_{16}\text{C}^{-1/0}$ clusters [39] are similar to those of $\text{Au}_{16}\text{Ge}^-$ and $\text{Au}_{16}\text{Sn}^-$

clusters [40], in which there are no dangling Au–X (X = C, Ge, and Sn) units. Another DFT study shows that an octahedral structure is predicted to be the global minimum of the gold-plated diamond, $C_5Au_{12}^-$, and may compete with the icosahedral shape for its cationic and neutral counterparts [41]. In 2009, Zaleski-Ejgierd and Pyykkö performed the bonding analysis for the simple aurocarbons [42], CAu_4 , C_2Au_2 , C_2Au_4 , C_2Au_6 , and C_6Au_6 , using DFT and the second-order Møller–Plesset perturbation theory (MP2). In addition, multiple-bond character can exist between Au and C atoms such as Cl_2AuCH [43], $AuCH_2^+$ [44,45], AuC^+ [46], $ClAuCH_2$ [47], $ClAuC$ [48], etc. Recently Wang et al. have probed the nature of the gold–carbon bonding in gold–alkynyl complexes [47], $LAu-CCH^{-1}$ (L = Cl, I, and CCH), in which the Au–C bond is to be one of the strongest Au–ligand bond as far as we know. In a DFT study on the structural pattern for $C_2Au_n^+$ ($n = 1, 3, 5$) and C_2Au_n ($n = 2, 4, 6$) dicarbon aurides [49], as clusters size increases, gold atoms serve as terminals and bridges in small dicarbon aurides, and form triangles when the number of gold atoms reaches four, additionally the H/Au analogy has been extended to H/ Au_3 analogy in this work. In 2014, the $AuC_2 \leftarrow AuC_2^-$ transition was investigated by Wang et al. using photoelectron spectroscopy (PES) and high-resolution PE imaging [50]. And the results show that the experimental spectrum is consistent with the bent AuC_2^- structure that is excited to a neutral state with a small or no change in Au–C–C bond angle and a ~ 0.08 Å change in the Au–C bond length. Due to the sp^3 hybridization of carbon atom, it maybe lead to large configuration change of gold cluster when the carbon atom interact with gold cluster. This will give us a good guide to discover and design novel material. Majumder and Kandalam have also proven that when gold clusters are doped with impurity elements possessing p electrons, the whole structure would prefer a three-dimensional (3D) configuration because of the sp^3 hybridization [20]. So, choosing the C-doped gold cluster maybe greatly change the catalytic performance of gold cluster.

Because there are relatively rare studies on the C-doped Au clusters, the present work will focus on the Au_nC ($n = 1-9$) clusters. The geometric constructions, relative stabilities, electronic stabilities, and electronic and magnetic properties have been investigated using DFT methods. The goal of this work is to investigate the Au–C interactions and to understand the growth mechanisms of the gold–carbon nanomaterials, as well as to get an insight into the influence of the valence state on the structures and physico-chemical properties.

2. Theoretical methods

The calculations are performed in three steps. First we used our modified Basin-Hopping (BH) algorithm [38,51–53] coupled with DFT in the DMol³ software package [54] to search the potential energy surfaces of the Au_nC ($n = 1-9$) clusters at the BLYP/DNP (DNP is the abbreviation of double-numerical polarized basis set) level of theory. Previous studies have indicated that the BLYP functional can reasonably describe the structure properties of carbon-gold system [47,49,50,55–58]. After the BH global search program, we chose a few tens of low-energy isomers for each size from several hundred searched structures. Then we ran the second step (optimization) implemented in the Gaussian 09 software package [59], in which the generalized gradient approximation (GGA) in the Perdew–Burke–Ernzerhof (PBE) functional form is used. All the low-lying structures are optimized at the PBE/6-31+G* level of theory, with the CRENBL effective core potential (ECP) plus corresponding basis set for Au atom. Next we selected a few low-lying isomers for further optimization at the PBE0/aug-cc-pVDZ (AVDZ, AVDZ is the valence double zeta polarization diffuse basis set) level of theory. In order to verify the stability of each isomer, we

calculated the harmonic vibrational frequency using the Gaussian 09 program at the same theoretical level with the optimization. If an imaginary vibrational mode appears, a relaxation along the coordinates of the imaginary vibrational mode will be performed until the true minimum is actually obtained. Moreover, the analysis of the harmonic vibrational frequency allows us to estimate the zero-point vibrational energy (ZPE) correction for every structure, so, all the energies in this work include the ZPE correction. Then we carried out the last step, single-point energy calculation, at the PBE0/aug-cc-pVTZ (AVTZ, AVTZ is the valence triple zeta polarization diffuse basis set) level of theory in Gaussian 09.

In the Au_nC clusters, the Au atoms account for a significant proportion compared to the C atom, so we can consider that the basis set of the Au atom is more critical for the accuracy of theoretical calculation. The PBE0 functional and CRENBL basis set can reasonably describe the structure and electron properties of gold cluster by previous studies [60–64]. We also test the reliabilities of different functionals for the optimization and single-point energy calculations, and it turns out that the PBE0 functional and CRENBL basis set is better than other functionals and basis set. The corresponding results are shown in Table S1. Thus, we select the PBE0/CRENBL group (AVDZ for the C atom) for optimization and PBE0/CRENBL (AVTZ for the C atom) group for the single-point energy calculation in the present work. Although it is difficult to confirm that we have achieved the most stable structures for the Au_nC ($n = 1-9$) clusters due to the lack of other theoretical and experimental data, we have performed an extensive search to the best of our ability.

3. Results and discussion

In order to investigate the effects of C dopant on pure gold clusters, we first performed some optimization and energy calculations on pure gold clusters, Au_{n+1} ($n = 1-9$), by using the same software, method, and basis set as in the Au_nC clusters. Only the lowest-energy structures of each size are chosen and shown in Figs. 1 and 2, and a few low-energy isomers are listed in Table S2. It is worth noting that the lowest-energy structures of Au_{n+1} ($n = 1-9$) cluster system are in great agreement with the previous results [20,22,28,65–71]. The averaged atomic binding energies, $E_b(n)$, attachment energies, $\Delta E(n)$, second-order difference of energies, $\Delta_2 E(n)$, vertical ionization potential, VIP, vertical electron affinity, VEA, chemical hardness, η , and the highest occupied-lowest unoccupied molecular orbital (HOMO–LUMO) gaps of pure gold clusters are also calculated and compared with the corresponding values of the Au_nC ($n = 1-9$) clusters. In addition, to provide effective guidelines for future experimental studies, we also calculated the vibrational frequencies for the lowest-energy structures of Au_nC ($n = 1-9$) clusters, which are listed in Table S3.

3.1. Structures

The lowest-energy structures of Au_nC and Au_{n+1} ($n = 1-5$) clusters along with a few low-lying isomers for doped gold clusters are listed in Fig. 1. The corresponding structures of Au_nC and Au_{n+1} ($n = 6-9$) clusters are shown in Fig. 2. According to the total energy from low to high, the low-lying isomers are designated by na , nb , nc , nd , ne , and nf , where n stands for the number of Au atoms in the clusters. At the same time, the symmetries and relative energies with respect to each of the corresponding global minimum are also presented in Figs. 1 and 2. In addition, the electronic energies for the lowest-energy structures of the Au_nC ($n = 1-9$) clusters are listed in Table S4, including the zero-point vibrational energies.

3.1.1. Structures of Au_nC ($n = 1-9$) clusters

The ground-state geometry of the AuC and Au_2C cluster are linear (1a, Fig. 1) and isosceles triangle (2a, Fig. 1) structure with C_{2v}

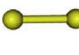
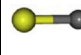

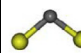

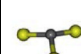
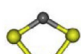
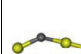

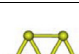

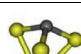
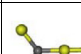
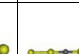
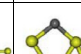




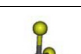





		-	-	-	-	-	-
Au ₂ D _{∞h}	1a, C _{∞v} 0.000	-	-	-	-	-	-
		-	-	-	-	-	-
Au ₃ D _{3h}	2a, C _{2v} 0.000	-	-	-	-	-	-
					-	-	-
Au ₄ C _{2v}	3a, C ₁ 0.000	3b, C _s 0.686	3c, C ₁ 0.708	3d, C ₁ 1.895	-	-	-
							
Au ₅ C _{2v}	4a, C ₁ 0.000	4b, C ₁ 0.396	4c, C ₁ 0.496	4d, C ₁ 1.143	4e, C ₁ 1.286	4f, C ₁ 1.493	4g, C ₁ 1.609
							
Au ₆ D _{3h}	5a, C ₁ 0.000	5b, C ₁ 0.028	5c, C ₁ 0.175	5d, C ₁ 0.179	5e, C ₁ 0.222	5f, C ₁ 0.453	5g, C ₁ 0.478

Fig. 1. Lowest-energy structures of Au_nC and Au_{n+1} ($n = 1-5$) clusters and a few low-lying isomers for doped clusters at the PBE0/AVTZ//PBE0/AVDZ level of theory. The first number represents the cluster size, n , and the data after the comma represent the geometry symmetries and the relative energies (zero-point vibrational energies included in eV) with respect to the ground state isomers for Au_nC ($n = 1-5$) clusters.


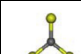
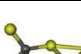

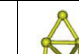

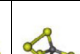



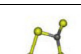

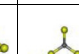




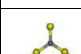







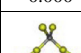

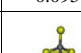
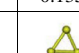
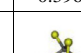


							
Au ₇ C _s	6a, C ₁ 0.000	6b, C ₁ 0.120	6c, C ₁ 0.476	6d, C ₁ 0.491	6e, C ₁ 0.492	6f, C ₁ 0.534	6g, C ₁ 0.563
							
Au ₈ D _{4h}	7a, C ₁ 0.000	7b, C ₁ 0.122	7c, C ₁ 0.288	7d, C ₁ 0.467	7e, C ₁ 0.518	7f, C ₁ 0.526	7g, C ₁ 0.529
							
Au ₉ C _{2v}	8a, C ₁ 0.000	8b, C ₁ 0.088	8c, C ₁ 0.095	8d, C ₁ 0.135	8e, C ₁ 0.396	8f, C ₁ 0.479	8g, C ₁ 0.496
							
Au ₁₀ D _{2h}	9a, C ₁ 0.000	9b, C ₁ 0.051	9c, C _s 0.214	9d, C ₁ 0.350	9e, C ₁ 0.367	9f, C ₁ 0.392	9g, C ₁ 0.395

Fig. 2. Lowest-energy structures of Au_nC and Au_{n+1} ($n = 6-9$) clusters and a few low-lying isomers for doped clusters at the PBE0/AVTZ//PBE0/AVDZ level of theory. The first number represents the cluster size, n , and the data after the comma represent the geometry symmetries and the relative energies (zero-point vibrational energies included in eV) with respect to the ground state isomers for Au_nC ($n = 6-9$) clusters.

symmetry, respectively. For the Au₃C cluster, a quasi-planar structure (3a, Fig. 1) is found to be the global minimum with the same Au–C bondlength of 1.94 Å, which is similar to the lowest-energy structures of the Au₃Si [26] and Au₃V [72] clusters. The reason for such non-planar structure in the Au_nC cluster is the directional covalent

bonding of Au and C atoms, which will be discussed in Section 3 by using the average ionic character of Au–C bond. Isomer 3a can be taken as Isomer 2a with another Au atom binding with the C atom.

In the case of Au₄C cluster, a distorted tetrahedron configuration (4a, Fig. 1) is proven to be the global minimum with the same

Au–C bond length of 1.97 Å, which can be described as Isomer 3a after another Au atom connecting to the C atom. Among the stable isomers of the Au₅C cluster, an isomer (5a, Fig. 1) with C₁ symmetry is proven to be the ground state, which derives from Isomer 4a with another Au atom top-capped. In addition, another derivative of Isomer 4a is Isomer 5b (Fig. 1) with only 0.028 eV higher in energy than Isomer 5a, and the small energy difference between these two isomers implies that a possible exchange of energy stability will appear at higher temperature or at a different theoretical level. If the Au₅ cluster is top-capped with a C atom, a new structure (5e, Fig. 1) will come into being, which can also be obtained by adding an Au atom to the edge of Isomer 4e, or by replacing an Au atom in the Au₆ cluster with a C atom. In addition, Isomer 5e is similar to the fourth most stable isomer of the Ag₅C cluster [23]. Finally, from Fig. 1, we can see that a few isomers of Au₅C cluster are found to be stable with very small energy difference, suggesting the existence of multiple nearly degenerate local minima in the potential energy surface. The lowest-energy structure of the Au₆C cluster can be seen as a subunit of Isomer 5e with the sixth Au atom connecting to the C atom, which has surprisingly planar configuration.

In our search for the global minimum of the Au₇C cluster, we find that the global minimum is a quasi-planar structure, in which the dopant atom is fourfold coordinated, and can derive from Isomer 6a (Fig. 2) by an added-Au atom connecting to the C atom. A planar structure (8a, Fig. 2) is found to be the most preferred structure for the Au₈C cluster with the C atom occupying the triply coordination site, and can be looked upon as Isomer 7c or 7d (Fig. 2) after another Au atom connecting to the C or Au atoms, respectively. Certainly, it can also derive from the Au₈ cluster by a dangling C–Au unit replacing one of the top Au atoms. As for the Au₉C cluster, the global minimum (9a, Fig. 2) is non-planar, which can be visualized as Isomer 8a with an added-Au atom binding with the C atom.

Combining Figs. 1 and 2, we can gain some important information about the most stable Au_nC and Au_{n+1} (n = 1–9) clusters which is summarized as follows:

(i) The most stable structures of Au_{n+1} (n = 1–9) clusters are planar at least up to n = 9, and the preference for planar structure is attributed to the strong relativistic effects [73–77], which enhance the s–d hybridization by stabilizing the 6s orbital and destabilizing the 5d orbital of the Au atom. The equilibrium geometries of C-doped Au clusters favor three-dimensional (3D) configuration for n = 4 and 5; quasi-2D configuration for n = 3, 7, and 9; 2D configuration for n = 6 and 8; and, as expected, 1D for Au₁C and 2D for Au₂C cluster. The C atom has four valence electrons and tends to bonding with four Au atoms, resulting in the 3D configuration with C occupying the fourfold coordination site, such as Au₄C and Au₅C clusters. As for the Au₇C and Au₉C clusters, similarly, the C atom occupies the fourfold coordination site, but the overall structures prefer for the quasi-2D configuration. This is because all the Au atoms that are not directly binding with the C atom remain the planar configuration, and that the extent of deviation from 2D configuration for the overall structure is smaller than that for the Au₄C and Au₅C clusters. It is surprising that the Au₆C and Au₈C clusters have planar structures with the C atoms occupying the triply coordinated sites, which is different from the Au₆C[−] and Au₈C[−] clusters [38].

(ii) The lowest-energy structures of Au_nC clusters are different from those of Au_{n+1} clusters, suggesting that the C dopant has significant influence on the structures of pure gold clusters. Furthermore, the C atom induces the local non-planarity while the rest of the structure continues to grow in a planar mode, which leads to an overall quasi-2D or 3D structure. In addition, compared with a C atom added to the Au_n cluster or a C atom replacing one Au

atom in the Au_{n+1} cluster, an Au atom added to the Au_{n−1}C cluster is the dominant growth pattern for Au_nC clusters.

(iii) Intuitively, the structures of Au_n clusters differ from those of their anionic counterparts, implying that the valence state exerts an effect on the structures of pure gold clusters. In addition, the structures of the Au_nC clusters are similar to those of the Au_nC[−] clusters, except for some fine distinctions about bondlength, bond angle, and symmetry. Thus the degree of similarity between the Au_nC and previously investigated Au_nC[−] clusters [38] is larger than that between the Au_n and Au_n[−] clusters, hinting that the valence state exerts a smaller effect on the C-doped gold clusters than on the pure gold clusters.

3.1.2. Compositions of HOMO

To gain insight on the geometric characteristics of these Au_nC clusters, the contributions of 5d, 6s, 6p orbitals of Au and 2s, 2p orbitals of C atoms to the HOMOs of Au_nC (n = 1–9) clusters have been calculated based on the natural bond orbital (NBO) analysis [78,79] in Gaussian 09. The corresponding values and histograms are shown in Table S5 and Fig. 3, respectively. For the Au atom, the 5d and 6s orbitals account for a large proportion of the HOMO, while the contribution of 6p orbital can be ignored, suggesting that the s–d orbital interaction exists in the Au atom and thus supports the relativistic effects. In addition, the contributions of 6s orbitals are larger than those of 5d orbitals to the HOMOs of Au_nC clusters except for the HOMO of AuC in α-spin (up) and the HOMOs of Au₈C and Au₉C in α-spin (up) and β-spin (down), implying that there exists significant s orbital character of Au atom in the frontier orbitals of C-doped Au clusters. As for the C atom, the 2p orbital takes up a big percentage of the HOMO with the ignored contribution of 2s orbital. To sum up, the HOMOs of Au_nC (n = 1–9) clusters mainly consist of the 5d, 6s orbitals of Au and 2p orbital of the C atom, which demonstrates that the chemical properties of Au_nC clusters are dominated by these three orbitals. As stated above, the gold clusters are doped with impurity elements possessing p electrons would prefer a 3D configuration because of the sp³ hybridization. We find that the C atom in the Au₄C, Au₅C and Au₉C clusters (in Figs. 1 and 2) form fourfold coordination site, and the percentage contribution of 6s orbitals of Au atom is always larger than the 2p orbitals of C atom to the highest occupied molecular orbital (HOMO). In contrast, the C atom occupies the triply coordinated site in the Au₂C, Au₃C, Au₆C, Au₇C, and Au₈C cluster (in Figs. 1 and 2), and forms a quasi-planar structure with the percentage contribution of 6s orbitals of Au atom, which is smaller than the 2p orbitals of C atom to the HOMO. So, the C-doped gold cluster maybe easily forms a 3D configuration when the percentage contribution of 6s orbitals of Au atom is larger than the 2p orbitals of C atom to the HOMO. The effects of the C atom on the stabilities

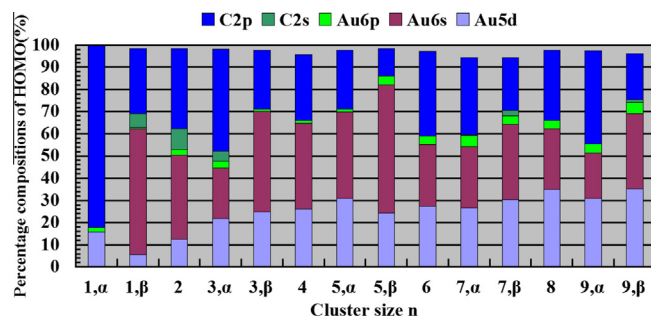


Fig. 3. Contributions (%) of 5d, 6s, 6p orbitals of Au atoms and 2s, 2p orbitals of C atoms to the highest occupied molecular orbital (HOMO) of Au_nC (n = 1–9) clusters. In addition, n, α is for the α-spin Au_nC (n = 1, 3, 5, 7, and 9) clusters, and n, β is for the β-spin Au_nC (n = 1, 3, 5, 7, and 9) clusters. The corresponding values are listed in Table S5.

and electronic and magnetic properties of pure gold clusters will be further discussed below.

3.2. Relative stabilities (thermodynamic stabilities)

To study the effects of C dopant on the relative stabilities (namely, thermodynamic stabilities) of pure gold clusters, the average atomic binding energies, $E_b(n)$, Au attachment energies, $\Delta_{Au}E(n)$, C attachment energies, $\Delta_C E(n)$, and the second-order difference of energies, $\Delta_2 E(n)$, for the lowest-energy structures of the $Au_n C$ and Au_{n+1} ($n = 1-9$) clusters are calculated. The corresponding values and curves of the $Au_n C$ ($n = 1-9$) clusters are shown in Table S4 and Fig. 4. In addition, the dissociation channels are also analyzed and shown in Fig. 5.

3.2.1. E_b , ΔE , $\Delta_2 E$

For the $Au_n C$ clusters, $E_b(n)$, $\Delta_{Au}E(n)$, $\Delta_C E(n)$, and $\Delta_2 E(n)$ are defined as follows:

$$E_b(n) = \frac{E(C) + nE(Au) - E(Au_n C)}{n + 1} \quad (1)$$

$$\Delta_{Au}E(n) = E(Au_{n-1}C) + E(Au) - E(Au_n C) \quad (2)$$

$$\Delta_C E(n) = E(Au_n) + E(C) - E(Au_n C) \quad (3)$$

$$\begin{aligned} \Delta_2 E(n) &= [E(Au_{n-1}C) + E(Au) - E(Au_n C)] - [E(Au_n C) + E(Au) - E(Au_{n+1}C)] \\ &= E(Au_{n-1}C) + E(Au_{n+1}C) - 2E(Au_n C) \end{aligned} \quad (4)$$

where $E(Au)$, $E(C)$, $E(Au_n)$, $E(Au_{n-1}C)$, $E(Au_n C)$, and $E(Au_{n+1}C)$ denote the total energies of the corresponding atoms and clusters including zero-point vibrational energies. For the Au_n clusters, the equation form of $E_b(n)$, $\Delta_{Au}E(n)$, and $\Delta_2 E(n)$ are the same as the above definition without C atom.

The $E_b(n)$, $\Delta_{Au}E(n)$, $\Delta_C E(n)$, and $\Delta_2 E(n)$ values for the lowest-energy structures of the $Au_n C$ and Au_{n+1} ($n = 1-9$) clusters against the number of Au atoms in clusters are plotted in Fig. 4. In Fig. 4(a), the average atomic binding energies of the $Au_n C$ clusters are larger than those of the corresponding Au_n clusters, suggesting that the addition of the C atom results in the integral improvement of the relative stabilities for the pure gold clusters. This is in line with the higher bond strength (shorter bond length) of Au–C than Au–Au bond. The enhanced-stability effect of the C atom is most outstanding between Au_2 and $Au_2 C$ clusters, whose binding energies are 0.98 eV and 7.20 eV, respectively. The average atomic binding energies of the $Au_n C$ clusters monotonously decrease with increasing size, while the binding energies of the Au_n clusters increase smoothly with the cluster size, n , going through a maximum of 1.69 eV at $n = 6$, and then following an odd–even alternation phenomenon in the little scope. No matter whether the average atomic binding energies of $Au_n C$ and Au_{n+1} ($n = 1-9$) clusters increase, they display a convergent tendency close to a limit. This means the larger the clusters, the smaller the enhanced-stability effect of C dopant, and this is in accordance with the doping ratio of C atom decreasing with the increasing size for the $Au_n C$ clusters.

As it is well known, in cluster physics, the attachment energies and the second-order difference of energies are sensitive quantities for the relative stabilities. The attachment energies of Au or C atom on the specific cluster size are on behalf of the ability towards single-atom dissociation. The corresponding attachment energy curves as a function of the number of Au atoms in clusters are shown in Fig. 4(b). It is clear that the interaction of C atom with the Au_n clusters is energetically more preferential than the Au atom with Au_{n-1} or $Au_{n-1}C$ clusters. That is to say, the dissociation of C atom from $Au_n C$ clusters requires more energy than that of Au atom from $Au_n C$ or Au_n clusters because the attachment energies of C are larger than those of Au, which reiterates the Au–C bond is

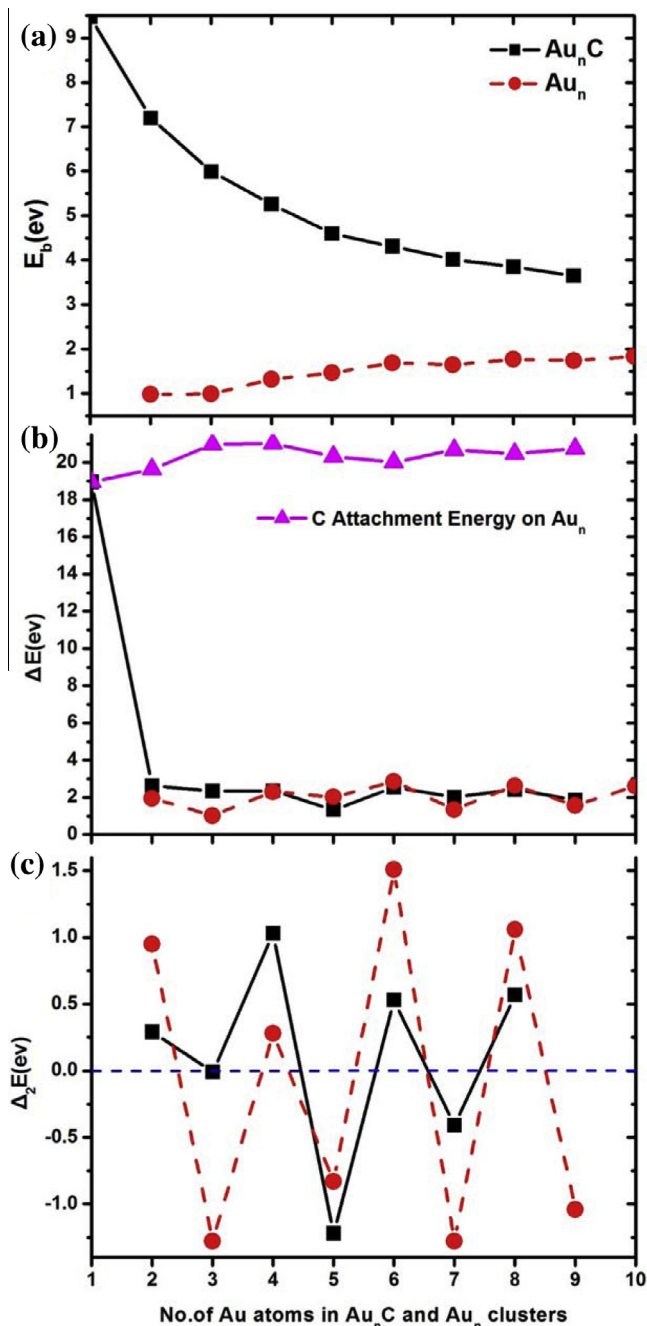


Fig. 4. Size dependence of the (a) average atomic binding energies of $Au_n C$ (black) and Au_n (red) clusters, $E_b(n)$, (b) Au attachment energies of $Au_n C$ (black) and Au_n (red) clusters (C attachment energies, $\Delta_C E(n)$, of $Au_n C$ clusters marked with the filled triangles (magenta)), $\Delta_{Au}E(n)$, and (c) the second-order difference energies of $Au_n C$ (black) and Au_n (red) clusters, $\Delta_2 E(n)$. (For interpretation of the references to color in this figure legend, the reader is referred to the web version of this article.)

stronger than the Au–Au bond. Au attachment energies on both $Au_n C$ and Au_n clusters depict a parity alternation trend, with n -even clusters having larger values than the adjacent n -odd ones excluding the $Au C$ cluster. The odd–even alternation phenomenon can be explained by the electron pairing effect. As for the $Au C$ cluster, the Au attachment energy is far greater than those of $Au_n C$ ($n = 2-9$) clusters, which is in good agreement with the average Au–C bond lengths and Wiberg bond indices (WBI) [80–82] of $Au_n C$ ($n = 1-9$) clusters in Table S4. The $Au C$ cluster has the smallest Au–C bond length (1.87 Å) and the largest WBI (1.458) in the full $Au_n C$ series, implying that the interaction of Au and C

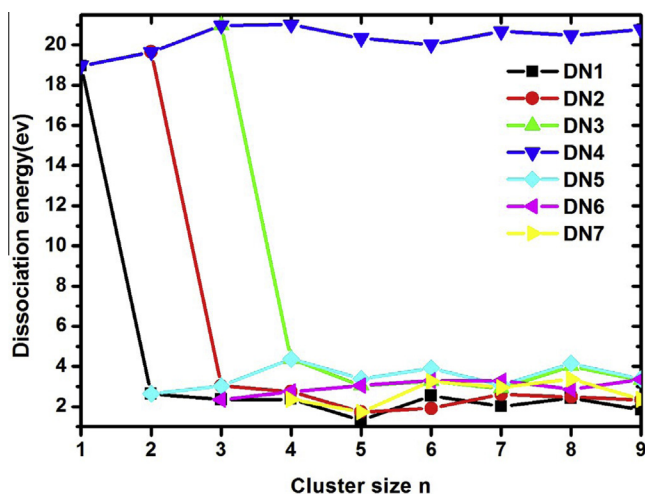


Fig. 5. Size dependence of the dissociation energies (zero-point vibrational energies included in eV) of the Au_nC ($n = 1-9$) clusters at the PBE0/AVTZ//PBE0/AVDZ level of theory. DN_x ($x = 1-7$) corresponds to different dissociation channels, as shown in the text.

atoms in AuC cluster is strongest, thus, there is no doubt that the AuC cluster has the largest attachment energy in spite of the odd number of electrons. Combined with Fig. 4(a), we can see that the C dopant can considerably enhance overall thermodynamic stabilities of pure gold clusters.

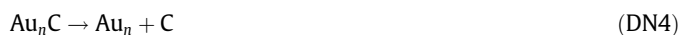
In addition, we also compared the Au attachment energies of Au_n and Au_nC clusters, and the results show that the dissociation of Au from Au_nC clusters requires more energies than that from Au_n clusters for $n = 2, 3, 4, 7$, and 9 . However, this trend is reversed for $n = 5, 6$, and 8 . For $n = 2, 3$, and 4 , the C atom binds with all the Au atoms in the corresponding clusters, and the dissociation of Au atom needs the rupture of Au–C bond, thus, there is no question of the higher energies for the dissociation of Au atom from these Au_nC clusters. As for the Au_7C and Au_9C clusters, in which the C atoms occupy the fourfold coordination site, the dissociation of Au atom also needs to break Au–C bond, and this is due to that the C atoms are triply coordinated in the dissociative products (Au_6C and Au_8C). Finally, the C attachment energy curve increases with increasing size and reaches maximum of 21.02 eV at the Au_4C cluster, and then presents an odd–even parity effect in range of $n = 5-9$. Hence, the Au_4C is the most stable cluster as for the C dissociation process.

The thermodynamic stability order in a series of clusters can also be demonstrated more definitely by the second-order difference of energies, $\Delta_2E(n)$, which can be construed as the difference between the Au attachment energies of the Au_nC and $Au_{n+1}C$ clusters, as shown in Eq. (4) [83]. The corresponding curves as a function of the number of Au atoms in both Au_nC and Au_n clusters are shown in Fig. 4(c). Both curves for these two kinds of clusters exhibit a clear odd–even oscillation with n -even clusters being more stable than the nearby n -odd ones. Moreover, the Au_4C and Au_6 clusters have the largest $\Delta_2E(n)$ values in corresponding series of clusters, suggesting that these two clusters are most stable from the point of relative stabilities and can be considered as the magic clusters. Particularly, the surprising stability [84] of Au_6 cluster can be further explained based on the structural planarity and six delocalized electrons being a magic number for the 2D systems.

Combined with Fig. 4(a)–(c), we can conclude that the enhanced-stability effect is more prominent for the situation of the dissociation of C atom than that of Au atom. As for the dissociation of Au atom, the incorporation of the C atom even decreases the thermodynamic stabilities of the $Au_{5,6,8}$ clusters. Because of their highest $\Delta_2E(n)$ values, the Au_4C and Au_6 clusters can be considered as magic numbers in their respective series.

3.2.2. Dissociation channel

The dissociation energies for all the possible channels based on the most stable structures of the Au_nC ($n = 1-9$) clusters are also calculated and exhibited in Fig. 5. All seven possible dissociation channels are listed in the following equations:



It can be seen from Fig. 5 that the dissociation energies of channel DN4 is far larger than those of the other channels, DN_x ($x = 2-7$), that is to say, it needs more energies for the C atom to be dissociated from the Au_nC ($n = 1-9$) clusters than the other atoms or units. In fact, the dissociation energies of DN4 are the C attachment energies. The change of dissociation energies of channel DN4 can be understood by their structure information. In general, the dissociation energies are proportional to the number of Au–C bond, which the number of Au–C bond increase from AuC to Au_4C (in Fig. 1). So, the dissociation energies reach the maximum value at Au_4C cluster for channel DN4. For the lowest-energy structure of Au_nC ($n = 3-9$) clusters, the Au_3C and Au_4C cluster can be seen as a basic unit when the $n > 4$. The dissociation energies of Au_nC ($n = 5-9$) clusters decrease with the added Au atom because the added Au atom can weaken the interaction of Au–C bond in the Au_3C or Au_4C cluster. So, the dissociation energies of channel DN4 firstly increase from $n = 1$ to $n = 4$, and then decrease from $n = 5$ to $n = 9$ in Table S4. The dissociation energies of DN_x ($x \neq 4$) is very close, and the corresponding values for DN1 is the lowest except for the defect at $n = 6$, where the dissociation energy of Au atom is larger than that of Au_2 unit. In general, the loss of the gold atom is the dominant dissociation pathway, with the Au atom and $Au_{n-1}C$ clusters as the main fragments.

3.3. Electronic stabilities (chemical stabilities)

To gain an insight into the influences of the C atom on the electronic stabilities (namely, chemical stabilities) of pure gold clusters, the VIP, VEA, η , and HOMO–LUMO gaps for the lowest-energy structures of Au_nC and Au_{n+1} ($n = 1-9$) clusters are calculated. The values of the Au_nC ($n = 1-9$) clusters are shown in Table S4, and the corresponding curves with the number of Au atoms in cluster are plotted in Figs. 6 and 7.

3.3.1. VIP, VEA, η

For the Au_nC clusters, VIP, VEA, and η are defined as follows:

$$VIP(n) = E(Au_nC)^+ - E(Au_nC) \quad (8)$$

$$VEA(n) = E(Au_nC) - E(Au_nC)^- \quad (9)$$

$$\eta(Au_nC) = \frac{VIP(n) - VEA(n)}{2} \quad (10)$$

where $E(Au_nC)^+$, $E(Au_nC)^-$, and $E(Au_nC)$ denote the total energies of the corresponding cationic, anionic, and neutral species based on the neutral geometries of the Au_nC clusters. For the Au_n clusters, VIP, VEA, and η are defined as follows:

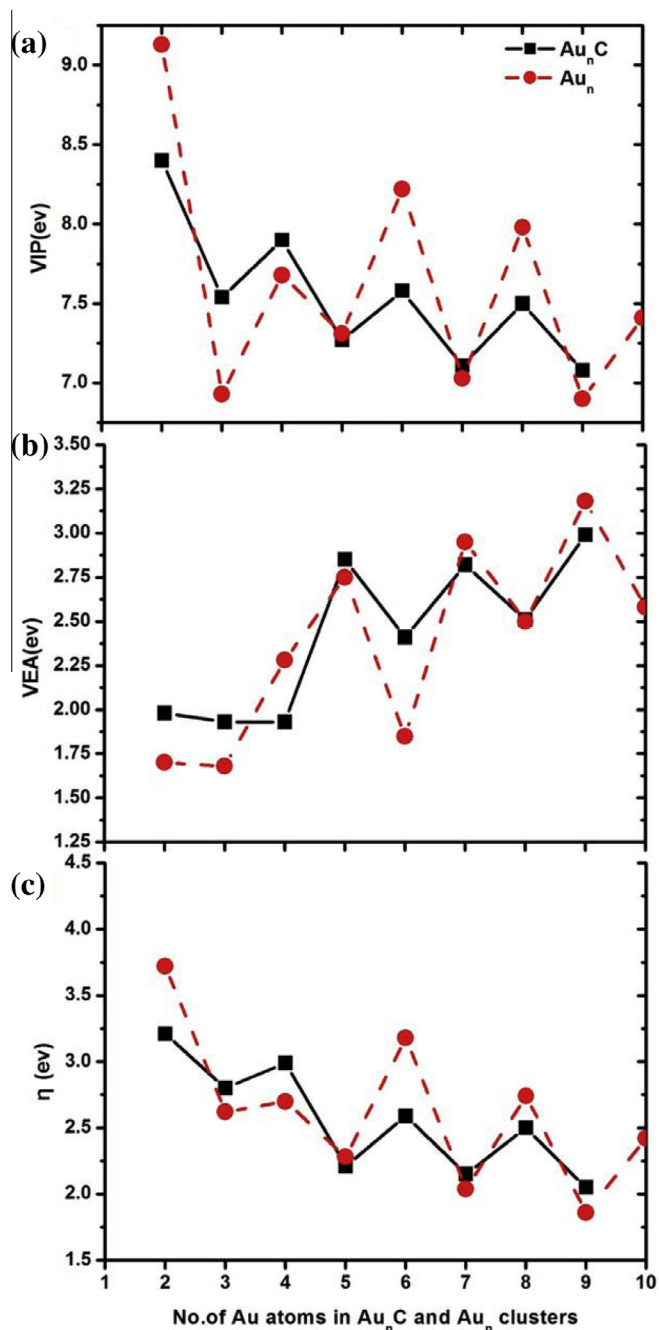


Fig. 6. Size dependence of the (a) vertical ionization potential, VIP, (b) vertical electron affinity, VEA, and (c) the chemical hardness, η , for the lowest-energy structures of Au_nC and Au_{n+1} ($n = 1-9$) clusters.

$$\text{VIP}(n) = E(\text{Au}_n^+) - E(\text{Au}_n) \quad (11)$$

$$\text{VEA}(n) = E(\text{Au}_n) - E(\text{Au}_n^-) \quad (12)$$

$$\eta(\text{Au}_n) = \frac{\text{VIP}(n) - \text{VEA}(n)}{2} \quad (13)$$

where $E(\text{Au}_n^+)$, $E(\text{Au}_n^-)$, and $E(\text{Au}_n)$ denote the total energies of the corresponding cationic, anionic, and neutral species based on the neutral geometries of the Au_n clusters.

The VIP, VEA, and η values for the lowest-energy structures of Au_nC and Au_{n+1} ($n = 1-9$) clusters against the number of Au atoms in clusters are plotted in Fig. 6. The VIP is calculated as the energy

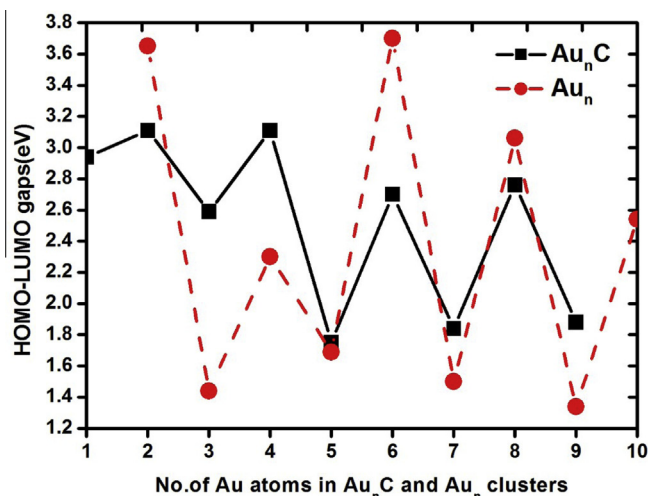


Fig. 7. Size dependence of the HOMO-LUMO gaps for the lowest-energy structures of Au_nC and Au_{n+1} ($n = 1-9$) clusters.

difference between the cationic and neutral species based on the global minimum of the neutral geometry, namely, the energies required to remove one electron from the neutral structure without any structural relaxation. The larger the VIP, the deeper the HOMO energy level, which results in higher chemical stability or less reactivity. It can be seen from Fig. 6(a) that the VIP's dependence on the cluster size shows a parity alternation trend with larger VIP values for the n -even Au_nC and Au_n clusters than the corresponding n -odd ones, implying that it is more difficult for the n -even Au_nC and Au_n clusters to lose an electron than the corresponding n -odd neighbors. This behavior can be explained by the electron pairing effect. Furthermore, the overall behaviors of the VIP curves for these two kinds of clusters as a function of the number of Au atoms have a nature of oscillatory decline with increasing cluster size except for the Au₃ and Au₄ clusters. The first two maximums for both Au_nC and Au_n clusters appear at Au₂C & Au₄C, and Au₂ & Au₆ clusters, respectively. So, we can say that these four clusters are relatively more stable than the other ones from the point of the ability to remove one electron. It is worthwhile noting that the VIP values of the Au_nC clusters are larger than those of Au_n clusters for $n = 3, 4, 7,$ and 9 , while the result is just the reverse for $n = 2, 5, 6,$ and 8 , which illustrates that the influences of the C atom on the chemical stabilities of pure gold clusters do not play a consistently enhancing or weakening role with different size.

VEA is another indicator for the evaluation of the chemical stability, which is defined as the energy difference between the neutral and anionic species based on the global minimum of neutral geometry. A smaller VEA value means that less energy is released to charge the neutral cluster with an extra electron. From Fig. 6(b), we realize that the VEA values for both Au_nC and Au_n clusters exhibit an odd-even alternation phenomenon with n -even Au_nC and Au_n clusters having smaller values than the corresponding adjacent n -odd ones with two exceptions of Au₃C and Au₃ clusters. Moreover, the overall trends for these two kinds of clusters are quivering upward with the increasing cluster size. There exist several relatively smaller values on the VEA curves, such as Au₃C, Au₄C, Au₃, Au₂, and Au₆ clusters, suggesting that these five clusters are relatively more stable chemically than the other sizes. In addition, the doped C atom can enhance the electronic stabilities of Au₄, Au₉, and Au₉ clusters due to the smaller VEA values, while the C atom reduces the electronic stabilities of the Au_n clusters for $n = 2, 3, 5, 6,$ and 8 . In order to understand the ability of gaining and losing electron of Au_nC ($n = 1-9$) clusters, we also calculate the adiabatic ionization potential (AIP) and adiabatic electron

affinity (AEA) of Au_nC ($n = 1-9$) clusters (in Table 1). The AIP is calculated as the energy difference between the cationic and neutral species based on their global minimum on the potential energy surface (PES), namely, the energies required to remove one electron from the neutral structure with structural relaxation. Table 1 shows a parity alternation trend with larger AIP values for the n -even Au_nC clusters than the corresponding n -odd ones, implying that it is more difficult for the n -even Au_nC clusters to lose an electron than the corresponding n -odd neighbors. AEA is defined as the energy difference between the neutral and anionic species based on their global minimum on the PES. The value of AEA also shows an odd–even alternation phenomenon with n -even Au_nC clusters having smaller values than the corresponding adjacent n -odd ones with two exceptions of AuC clusters in Table 1. A smaller AEA value means that it is easy to gain an extra electron. So, Table 1 shows the Au_nC clusters for $n = \text{even}$ are more easily to gain an electron than the corresponding $n = \text{odd}$ neighbors. The natural population analysis (NPA) can provide a reasonable explanation for the localization of natural charge in clusters, and we calculate the natural atomic charge population of C atom for Au_nC and Au_nC^- ($n = 1-9$) clusters in Table 1. As shown in Table 1, the atomic charges of C atom are negative for Au_nC ($n = 1-9$) clusters and Au_nC^- ($n = 3-9$) clusters except for Au_nC^- ($n = 1, 2$) clusters, indicating that the charges in the corresponding clusters mainly transfer from the Au_n^- host to the C atom owing to the larger electronegativity of C than that of Au. The average Au–C bond length of Au_nC ($n = 1-9$) clusters is small than the Au_nC^- ($n = 1-9$) clusters. The reason maybe is that the transfer amount of electron of the Au_nC^- ($n = 1-9$) clusters from the Au_n^- host is less than Au_nC ($n = 1-9$) clusters with an extra electron for Au_nC^- ($n = 1-9$) clusters. This will weaken the interaction of Au–C bond and increase the distance of Au–C bond in the Au_nC^- ($n = 1-9$) clusters.

In the frame of DFT, according to the principle of maximum hardness (PMH) [85,86], absolute chemical hardness, η , of the equilibrium state of an electronic system is rigorously defined as the second derivative of the total energy (E) with respect to the number of electrons (N),

$$\eta = \frac{1}{2} \left(\frac{\partial^2 E}{\partial N^2} \right)_{V(\mathbf{r})} = \frac{1}{2} \left(\frac{\partial \mu}{\partial N} \right)_{V(\mathbf{r})} \quad (14)$$

where μ is the electronic chemical potential (constant through the system), and $V(\mathbf{r})$ is the potential acting on an electron at \mathbf{r} due to the nuclear attraction plus such other external forces as may be present. In addition, in the case of molecular orbital theory, the Koopmans' theorem [87] regards the VIP and VEA as the opposite number of the eigenvalues of the HOMO and LUMO. However, the theorem is not fit for species with a negligible HOMO–LUMO energy gap or when it is required to consider the influence of other orbitals

Table 1

The compare of natural population analysis (NPA) of C atoms in the lowest-energy structure of Au_nC and Au_nC^- ($n = 1-9$) clusters; the adiabatic ionization potential (AIP) and adiabatic electron affinity (AEA) of Au_nC ($n = 1-9$) clusters.

Cluster size	NPA (Au_nC) ^a	NPA (Au_nC^-) ^b	AIP (eV)	AEA (eV)
$n = 1$	−0.085	−0.817	8.938	0.639
$n = 2$	−0.396	−0.859	7.809	2.004
$n = 3$	−1.014	−1.169	7.056	2.310
$n = 4$	−1.627	−1.604	7.551	1.953
$n = 5$	−1.435	−1.543	6.561	3.277
$n = 6$	−0.823	−1.106	7.486	2.525
$n = 7$	−1.361	−1.657	6.950	3.081
$n = 8$	−0.808	−1.060	7.364	2.696
$n = 9$	−1.348	−1.621	6.885	3.323

^a NPA is obtained from the NBO analysis in Gaussian 09.

^b The lowest-energy structures are obtained from Ref. [38].

including the HOMO and LUMO. On the basis of a finite-difference approximation and the above Koopmans' theorem, the chemical hardness is simplified and shown in Eqs. (10) and (13).

The chemical hardness for the lowest-energy structures of the Au_nC and Au_n clusters are calculated and plotted in Fig. 6(c). It is easy to be found that the η curves for both Au_nC and Au_n clusters present a similar odd–even alternation phenomenon with n -even Au_nC and Au_n clusters being more stable than the adjacent n -odd ones. And the overall trends for these two kinds of clusters are declining with oscillation except for the Au_4 cluster. It is worth mentioning that the Au_2C , Au_4C , Au_2 , and Au_6 clusters have higher chemical hardness than the others, hinting that these four clusters are more stable chemically from a comprehensive perspective of the abilities to lose and obtain an electron. Thus, these four clusters can also be called the “hard molecule” because of their higher chemical hardness. In addition, the chemical hardness of Au_nC clusters is larger than that of the corresponding Au_n clusters for $n = 3, 4, 7$, and 9 , suggesting that the addition of the C atom enhances the chemical stabilities of these pure gold clusters, on the contrary, the C atom decreases the chemical stabilities of the Au_2 , Au_5 , Au_6 , and Au_8 clusters.

3.3.2. HOMO–LUMO gap

The electronic stabilities of the Au_nC and Au_n clusters can also be discussed in another electronic quantity called HOMO–LUMO gap, which reflects the ability for electrons to jump from the highest occupied to the lowest unoccupied molecular orbital, as well as the ability for molecule to participate in the chemical reactions to a certain extent. A large gap value stands for a high chemical stability. The corresponding gaps for Au_nC and Au_n clusters are plotted in Fig. 7. The gap's dependences on the cluster size for these two kinds of clusters present an oscillation between the clusters with even and odd electrons. To be specific, the n -even Au_nC and Au_n clusters have higher gaps, namely, higher chemical stabilities, than n -odd ones. The gap curves reach relatively large values at Au_2C , Au_4C , Au_2 , and Au_6 clusters, revealing that these four clusters are relatively more stable than the other sizes. The introduction of the C atom improves the chemical stabilities of the $Au_{3,4,5,7,9}$ clusters, in particular, the enhanced-stability effect is most outstanding for the unit of Au_4 and Au_4C clusters. In contrast, there is negative enhanced-stability effect for the $Au_{2,6,8}$ clusters after the addition of the C atom.

In the present work, it must be mentioned that although all the energy parameters of VIP, VEA, η , and the HOMO–LUMO gap can serve as the indicators for the chemical stabilities, they reflect the stabilities of different aspects. To be specific, VIP characterizes the ability for the neutral species to lose an electron, VEA describes the ability to obtain an electron, and the HOMO–LUMO gap reflects the ability for an electron to jump from the HOMO to the LUMO. Thus, it is not necessary for these energy parameters to possess a consistent conclusion about the chemical stabilities. But for the Au_nC and Au_{n+1} ($n = 1-9$) clusters in this work, we can draw a confirm conclusion that the Au_2C , Au_4C , Au_2 , and Au_6 clusters are relatively more stable chemically than the other sizes. At last, combining an analysis of the relative and electronic stabilities, we think the Au_4C and Au_6 clusters can be regarded as the building blocks of the novel material because of their higher relative and electronic stabilities.

3.4. Electronic and magnetic properties

In order to understand the electronic and magnetic properties of the Au_nC and Au_{n+1} ($n = 1-9$) clusters, the detailed natural population analysis (NPA), natural electronic configuration (NEC), and magnetic moments for the lowest-energy structures are discussed based on the NBO analysis [78,79] in Gaussian 09.

3.4.1. Electronic properties

The charges of 5d, 6s, 6p orbitals of Au atoms and 2s, 2p orbitals of C atoms, along with the atomic charges of C atoms for the global minimums of the Au_nC and Au_{n+1} ($n = 1-9$) clusters are shown in Table S6. The charges on the C atoms in the Au_nC clusters are negative, indicating that the charges in the corresponding clusters transfer from the Au_n host to the C atom due to the larger electronegativity of C (2.55) than that of Au (2.4). To analyze the bonding property between Au and C atoms, we also calculated the average ionic character of Au–C bond for each kind of clusters based on the NBO analysis, and the ionicity of the Au–C bond is defined as follows:

$$i_{Au,C} = \left| \frac{C_{Au}^2 - C_C^2}{C_{Au}^2 + C_C^2} \right| \quad (15)$$

where C_{Au} and C_C denote the polarization coefficients of Au and C atoms, respectively. The average ionicity of Au–C bond in the Au_nC ($n = 1-9$) clusters are 11.99%, 29.93%, 26.62%, 38.14%, 38.03%, 42.21%, 38.59%, 40.64%, and 34.08%, respectively, all of which are less than 50%. So, Au and C atoms interact with each other mostly via covalent bond rather than ionic bond, which can also be confirmed through the difference in electronegativity, Δ_{EN} . Covalently bonded interactions will exist in clusters if $\Delta_{EN} < 1.7$, and $\Delta_{EN} = 0.15$ for Au_nC clusters.

In order to further understand the charge transfer, the internal charge populations of C and Au atoms are also considered by NEC analysis. As for the free Au and C atoms, the distributions of valence electrons are $5d^{10}6s^1$ and $2s^22p^2$, respectively. We first consider the charge population in Au atom of the pure gold clusters. As shown in Table S6, the 5d and 6s orbitals lose 0.050–0.121 and 0.015–0.064 electrons, respectively, and the 6p orbital gains a certain amount of charge ranging from 0.020 to 0.176. Moreover, a more detailed analysis reveals that the 5d orbital serves as the major contributor for the charge transfer. It is worth noting that the 6s orbitals of Au_2 and Au_3 clusters receives 0.030 and 0.003 electrons, respectively, which differs from the other sizes of gold clusters. When the C atom is introduced into the pure gold clusters, the NEC analysis exhibits that the 2s orbital loses 0.090–0.510 electrons, while the 2p orbital receives 0.150–2.060 electrons, with the 3s and 3p orbitals gaining negligible charges. With regard to the internal charge transfer in the Au atom of the Au_nC clusters, the NEC analysis shows that the charge transfer occurs from 5d and 6s orbitals to 6p orbital with a certain amount of electrons. What is noteworthy to say is that the 6s orbitals of Au_1C and Au_2C clusters receives 0.320 and 0.160 electrons, respectively, which differs from the other C-doped gold clusters. Similar to the case of the pure gold clusters, the 5d orbital is the major contributor for the charge transfer. In addition, due to the incorporation of the C atom, the electron populations of the 5d, 6s, and 6p orbitals of the Au atom have been changed. More specifically, the charges of 5d orbital decrease after the addition of the C atom. As for the 6s and 6p orbitals, the corresponding charges change little and there is not obvious trend of increase or decrease being observed.

3.4.2. Magnetic properties

We also analyzed the magnetic properties for the lowest-energy structures of the Au_nC and Au_{n+1} ($n = 1-9$) clusters. The total magnetic moments for these two kinds of clusters, and the local magnetic moments on the C atom are shown in Table S7 and plotted in Fig. 8. The total magnetic moment's dependence on the cluster size exhibits a clear odd–even oscillation. Moreover, both doped and pure gold clusters with even-number valence electrons have null magnetic moment owing to an equal number of spin-up and spin-down occupied valence states. However, for the odd ones, the total magnetic moments for these clusters are less than but

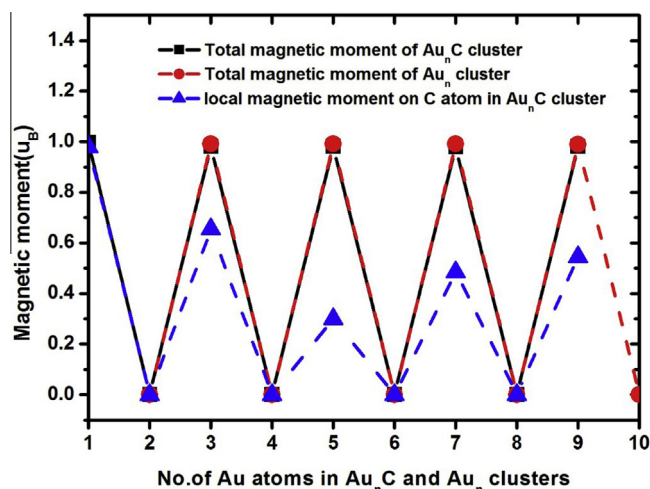


Fig. 8. Size dependence of the total magnetic moments for the lowest-energy structures of Au_nC and Au_{n+1} ($n = 1-9$) clusters, and the local magnetic moments on the C atoms in the corresponding Au_nC ($n = 1-9$) clusters.

close to $1 \mu_B$, which is because that the contributions of excited states to the electron spin magnetic moment are not taken into account. In addition, the magnetic moments on the C atoms of the Au_nC clusters also demonstrate the odd–even alternation phenomenon, with the local magnetic moments of zero for the n -even clusters. For the n -odd ones, the magnetic moments on the C atoms decrease and then increase, with the minimal value at the Au_5C ($n = \text{odd}$) clusters. Additionally, the total magnetic moments of the Au_nC ($n = \text{odd}$) clusters are largely located on the C atoms for the Au_1C , Au_3C , and Au_9C clusters while on the Au_n host for the Au_5C and Au_7C clusters.

Furthermore, Table S7 displays the magnetic moments of 5d, 6s, 6p orbitals of Au atoms and 2s, 2p orbitals of the C atoms for the Au_nC and Au_{n+1} ($n = 1-9$) clusters. The local magnetic moments of the C atom mostly concentrate upon 2p orbital, whereas the 5d and 6s orbitals play a big part in the magnetic moments of the Au atoms in the Au_nC clusters. And the distribution of the magnetic moment within the Au atom reflects the s-d orbital hybridization from another perspective, which roots in the so-called relativistic effects.

4. Conclusions

The geometric constructions, relative stabilities, electronic stabilities, and electronic and magnetic properties of the Au_nC and Au_{n+1} ($n = 1-9$) clusters have been investigated using hyper-GGA in PBE0 functional form in the Gaussian 09 software package. All the results are summarized as follows:

1. One Au atom added to the $Au_{n-1}C$ cluster is the dominant growth pattern for Au_nC clusters. The most stable structures of Au_{n+1} clusters are planar at least up to $n = 9$. The C dopant induces the local non-planarity and results in an over-all quasi-2D or 3D configuration. Thus, the C atom can vary the ground-state structures of the pure gold clusters. In addition, the valence state exerts a smaller effect on the structures of C-doped gold clusters than on the pure gold clusters. An analysis on the percentage compositions of the HOMOs of the Au_nC clusters demonstrates that the chemical properties of the C-doped Au clusters are dominated by 5d, 6s orbitals of Au and 2p orbital of the C atom.
2. The higher atomic binding energies of Au_nC over Au_n ($n = 1-9$) clusters reflect that the addition of the C atom can improve the integral relative stabilities of the pure gold clusters, and

the enhanced-stability effect is more prominent for the situation of the dissociation of C atom than that of the Au atom. As for the dissociation of Au atom, the incorporation of the C atom even decreases the thermodynamic stabilities of the Au_{5,6,8} clusters. Because of their highest $\Delta_2E(n)$ values, the Au₄C and Au₆ clusters can be considered as magic numbers in their respective series. The study on the dissociation channels of the Au_nC ($n = 1-9$) clusters indicates that the loss of the Au atom is the dominant dissociation pathway, with the Au atom and Au_{n-1}C clusters as the main fragments.

- The electronic stabilities of the Au_nC and Au_{n+1} ($n = 1-9$) clusters are discussed based on the energy parameters of VIP, VEA, η , and the HOMO–LUMO gap. And we can draw a confirm conclusion that the Au₂C, Au₄C, Au₂, and Au₆ clusters are relatively more stable chemically than the other sizes. Through a comprehensive consideration of the relative and electronic stabilities, we can conclude that the Au₄C and Au₆ clusters can be regarded as the magic clusters.
- The electronic and magnetic properties for the lowest-energy structures of the Au_nC and Au_{n+1} ($n = 1-9$) clusters are discussed based on the NBO analysis. The NPA shows that the charges in the Au_nC clusters transfer from the Au_n host to the C atom. The Au and C atoms interact with each other mostly via covalent bond rather than ionic bond. In addition, the NEC analysis indicates that the charges transfer from 2s orbital to the 2p orbital in the C atom and from the 5d, 6s orbitals to the 6p orbital in the Au atom of the Au_nC clusters, with the 5d orbital serving as the major contributor for the charge transfer. The situation in the Au_{n+1} clusters is similar to that in the Au_nC clusters. The total magnetic moments of the Au_nC and Au_n ($n = \text{odd}$) clusters are less than but close to 1 μ_B , with the total magnetic moments of the Au_nC ($n = \text{odd}$) clusters mainly locating on the C atoms for Au_{1,3,9}C and on the Au_n host for $n = 5$ and 9. However, the total magnetic moments of the Au_nC and Au_n ($n = \text{even}$) clusters are zero. In addition, the magnetic moments of the Au atoms in Au_nC and Au_n ($n = \text{odd}$) clusters mainly focus on the 5d and 6s orbitals. As for the C atom, the magnetic moments mostly concentrate upon the 2p orbital.

Conflict of interest

No conflict of interest.

Acknowledgments

The study was supported by grants from the National Natural Science Foundation of China (Grant Nos. 21403244, 21133008, 41505114, 21573241 and 41527808), Director Foundation of AIOFM (AGHH201505, Y23H161131), the National High Technology Research and Development Program of China (863 Program) (Grant No. 2014AA06A501), and the program of Formation Mechanism and Control Strategies of Haze in China (Grant No. XDB05000000). Acknowledgement is also made to the “Thousand Youth Talents Plan”, Scientific Research Equipment Development Program (YZ201422) and “Interdisciplinary and Cooperative Team” of CAS. The computation was performed in EMSL, a national scientific user facility sponsored by the department of Energy’s Office of Biological and Environmental Research and located at Pacific Northwest National Laboratory (PNNL). PNNL is a multiprogram national laboratory operated for the DOE by Battelle. Part of the computation was performed at the Supercomputing Center of USTC.

Appendix A. Supplementary data

Supplementary data associated with this article can be found, in the online version, at <http://dx.doi.org/10.1016/j.chemphys.2016.03.009>.

References

- [1] P. Pyykkö, *Angew. Chem. Int. Ed.* 43 (2004) 4412.
- [2] P. Pyykkö, *Inorg. Chim. Acta* 358 (2005) 4113.
- [3] P. Pyykkö, *Chem. Soc. Rev.* 37 (2008) 1967.
- [4] B. Wang, X. Xiao, X. Huang, P. Sheng, J. Hou, *Appl. Phys. Lett.* 77 (2000) 1179.
- [5] J. Hou, B. Wang, J. Yang, X. Wang, H. Wang, Q. Zhu, X. Xiao, *Phys. Rev. Lett.* 86 (2001) 5321.
- [6] C. Kiely, J. Fink, M. Brust, D. Bethell, D. Schiffrin, *Nature* 396 (1998) 444.
- [7] C.L. Cleveland, U. Landman, T.G. Schaaff, M.N. Shafiqullin, P.W. Stephens, R.L. Whetten, *Phys. Rev. Lett.* 79 (1997) 1873.
- [8] A.P. Alivisatos, K.P. Johnsson, X. Peng, T.E. Wilson, C.J. Loweth, M.P. Bruchez, P. G. Schultz, *Nature* 382 (1996) 609.
- [9] C.A. Mirkin, R.L. Letsinger, R.C. Mucic, J.J. Storhoff, *Nature* 382 (1996) 607.
- [10] M. Valden, X. Lai, D.W. Goodman, *Science* 281 (1998) 1647.
- [11] B. Yoon, H. Häkkinen, U. Landman, A.S. Wörz, J.-M. Antonietti, S. Abbet, K. Judai, U. Heiz, *Science* 307 (2005) 403.
- [12] C. Zhang, B. Yoon, U. Landman, *J. Am. Chem. Soc.* 129 (2007) 2228.
- [13] M.-C. Daniel, D. Astruc, *Chem. Rev.* 104 (2004) 293.
- [14] M. Haruta, *Catal. Today* 36 (1997) 153.
- [15] N.L. Rosi, C.A. Mirkin, *Chem. Rev.* 105 (2005) 1547.
- [16] E. Katz, I. Willner, *Angew. Chem. Int. Ed.* 43 (2004) 6042.
- [17] C. Burda, X. Chen, R. Narayanan, M.A. El-Sayed, *Chem. Rev.* 105 (2005) 1025.
- [18] M. Haruta, *Nature* 437 (2005) 1098.
- [19] R. Pal, S. Bulusu, X. Zeng, *J. Comput. Methods Sci. Eng.* 7 (2007) 185.
- [20] C. Majumder, A.K. Kandalam, P. Jena, *Phys. Rev. B* 74 (2006) 205437.
- [21] Z. Zhang, B. Cao, H. Duan, *J. Mol. Struct.: Theochem.* (2008) 22.
- [22] M. Zhang, S. Chen, Q. Deng, L. He, L. Zhao, Y. Luo, *Eur. Phys. J. D* 58 (2010) 117.
- [23] F.Y. Naumkin, *Comput. Theor. Chem.* 1021 (2013) 191.
- [24] L. Gagliardi, *J. Am. Chem. Soc.* 125 (2003) 7504.
- [25] B. Kiran, X. Li, H.J. Zhai, L.F. Cui, L.S. Wang, *Angew. Chem.* 116 (2004) 2177.
- [26] C. Majumder, *Phys. Rev. B* 75 (2007) 235409.
- [27] D. Yuan, Y. Wang, Z. Zeng, *J. Chem. Phys.* 122 (2005) 114310.
- [28] S.J. Wang, X.Y. Kuang, C. Lu, Y.F. Li, Y.R. Zhao, *Phys. Chem. Chem. Phys.* 13 (2011) 10119.
- [29] K. Koyasu, M. Mitsui, A. Nakajima, K. Kaya, *Chem. Phys. Lett.* 358 (2002) 224.
- [30] X. Li, B. Kiran, L.-F. Cui, L.-S. Wang, *Phys. Rev. Lett.* 95 (2005) 253401.
- [31] M. Torres, E. Fernández, L. Balbás, *Phys. Rev. B* 71 (2005) 155412.
- [32] K. Koyasu, Y. Naono, M. Akutsu, M. Mitsui, A. Nakajima, *Chem. Phys. Lett.* 422 (2006) 62.
- [33] S. Neukermans, E. Janssens, H. Tanaka, R. Silverans, P. Lievens, *Phys. Rev. Lett.* 90 (2003) 033401.
- [34] K.-M. Xu, T. Huang, H. Wen, Y.-R. Liu, Y.-B. Gai, W.-J. Zhang, W. Huang, *RSC Adv.* 3 (2013) 24492.
- [35] Y. Li, Y. Cao, Y. Li, S. Shi, X. Kuang, *Eur. Phys. J. D* 66 (2012) 10.
- [36] Y. Hua, Y. Liu, G. Jiang, J. Du, J. Chen, *J. Phys. Chem. A* 117 (2013) 2590.
- [37] Y.-F. Li, Y. Li, X.-Y. Kuang, *Eur. Phys. J. D* 67 (2013) 132.
- [38] L.-L. Yan, Y.-R. Liu, T. Huang, S. Jiang, H. Wen, Y.-B. Gai, W.-J. Zhang, W. Huang, *J. Chem. Phys.* 139 (2013) 244312.
- [39] W. Fa, A. Yang, *Phys. Lett. A* 372 (2008) 6392.
- [40] L.-M. Wang, S. Bulusu, W. Huang, R. Pal, L.-S. Wang, X.C. Zeng, *J. Am. Chem. Soc.* 129 (2007) 15136.
- [41] F. Naumkin, *Phys. Chem. Chem. Phys.* 8 (2006) 2539.
- [42] P. Zaleski-Ejgierd, P. Pyykkö, *Can. J. Chem.* 87 (2009) 798.
- [43] P. Pyykkö, T. Tamm, *Theor. Chem. Acc.* 99 (1998) 113.
- [44] K.K. Irikura, W.A. Goddard III, *J. Am. Chem. Soc.* 116 (1994) 8733.
- [45] H. Schwarz, *Angew. Chem. Int. Ed.* 42 (2003) 4442.
- [46] M. Barysz, P. Pyykkö, *Chem. Phys. Lett.* 285 (1998) 398.
- [47] H.-T. Liu, X.-G. Xiong, P.D. Dau, Y.-L. Wang, D.-L. Huang, J. Li, L.-S. Wang, *Nat. Commun.* 4 (2013) 2223.
- [48] C. Puzzarini, K.A. Peterson, *Chem. Phys.* 311 (2005) 177.
- [49] D.-Z. Li, S.-D. Li, J. Cluster Sci. 22 (2011) 331.
- [50] I. León, Z. Yang, L.-S. Wang, *J. Chem. Phys.* 140 (2014) 084303.
- [51] Y.-R. Liu, H. Wen, T. Huang, X.-X. Lin, Y.-B. Gai, C.-J. Hu, W.-J. Zhang, W. Huang, *J. Phys. Chem. A* 118 (2014) 508.
- [52] H. Wen, Y.-R. Liu, T. Huang, K.-M. Xu, W.-J. Zhang, W. Huang, L.-S. Wang, *J. Chem. Phys.* 138 (2013) 174303.
- [53] S. Jiang, Y.R. Liu, T. Huang, H. Wen, K.M. Xu, W.X. Zhao, W.J. Zhang, W. Huang, *J. Comput. Chem.* 35 (2014) 159.
- [54] B. Delley, *J. Chem. Phys.* 92 (1990) 508.
- [55] P. Pyykkö, M. Patzschke, J. Suurpere, *Chem. Phys. Lett.* 381 (2003) 45.
- [56] Z. Yang, I. León, L.-S. Wang, *J. Chem. Phys.* 139 (2013) 021106.
- [57] X. Sun, J. Du, G. Jiang, *Struct. Chem.* 24 (2013) 1289.
- [58] B. Ticknor, B. Bandyopadhyay, M. Duncan, *J. Phys. Chem. A* 112 (2008) 12355.
- [59] M.J. Frisch, G.W. Trucks, H.B. Schlegel, G.E. Scuseria, M.A. Robb, J.R. Cheeseman, G. Scalmani, V. Barone, B. Mennucci, G.A. Petersson, H. Nakatsuji, M. Caricato,

- X. Li, H.P. Hratchian, A.F. Izmaylov, J. Bloino, G. Zheng, J.L. Sonnenberg, M. Hada, et al., Gaussian 09, Revision A.02, Gaussian Inc, Wallingford, CT, 2009.
- [60] W. Huang, R. Pal, L.-M. Wang, X.C. Zeng, L.-S. Wang, *J. Chem. Phys.* 132 (2010) 054305.
- [61] N. Shao, W. Huang, Y. Gao, L.-M. Wang, X. Li, L.-S. Wang, X.C. Zeng, *J. Am. Chem. Soc.* 132 (2010) 6596.
- [62] R. Pal, L.-M. Wang, W. Huang, L.-S. Wang, X.C. Zeng, *J. Chem. Phys.* 134 (2011) 054306.
- [63] N. Shao, W. Huang, W.-N. Mei, L.S. Wang, Q. Wu, X.C. Zeng, *J. Phys. Chem. C* 118 (2014) 6887.
- [64] B. Schaefer, R. Pal, N.S. Khetrpal, M. Amsler, A. Sadeghi, V. Blum, X.C. Zeng, S. Goedecker, L.-S. Wang, *ACS Nano* 8 (2014) 7413.
- [65] C. Majumder, S. Kulshreshtha, *Phys. Rev. B* 73 (2006) 155427.
- [66] Y.-F. Li, A.-J. Mao, Y. Li, X.-Y. Kuang, *J. Mol. Model.* 18 (2012) 3061.
- [67] H.M. Lee, M. Ge, B. Sahu, P. Tarakeshwar, K.S. Kim, *J. Phys. Chem. B* 107 (2003) 9994.
- [68] E.M. Fernández, J.M. Soler, I.L. Garzón, L.C. Balbás, *Phys. Rev. B* 70 (2004) 165403.
- [69] X.-J. Kuang, X.-Q. Wang, G.-B. Liu, *J. Alloys Compd.* 570 (2013) 46.
- [70] L. Cheng, K. Xiao-Yu, L. Zhi-Wen, M. Ai-Jie, M. Yan-Ming, *J. Phys. Chem. A* 115 (2011) 9273.
- [71] B. Assadollahzadeh, P. Schwerdtfeger, *J. Chem. Phys.* 131 (2009) 064306.
- [72] D. Dong, Z. Ben-Xia, Z. Bing, *Mol. Phys.* 109 (2011) 1709.
- [73] P. Schwerdtfeger, *Heteroat. Chem.* 13 (2002) 578.
- [74] P. Schwerdtfeger, *J. Am. Chem. Soc.* 111 (1989) 7261.
- [75] P. Schwerdtfeger, P.D. Boyd, A.K. Burrell, W.T. Robinson, M.J. Taylor, *Inorg. Chem.* 29 (1990) 3593.
- [76] P. Schwerdtfeger, P.D. Boyd, S. Brienne, A.K. Burrell, *Inorg. Chem.* 31 (1992) 3411.
- [77] R. Wesendrup, J.K. Laerdahl, P. Schwerdtfeger, *J. Chem. Phys.* 110 (1999) 9457.
- [78] A.E. Reed, L.A. Curtiss, F. Weinhold, *Chem. Rev.* 88 (1988) 899.
- [79] A.E. Reed, F. Weinhold, *J. Chem. Phys.* 78 (1983) 4066.
- [80] I. Mayer, *Chem. Phys. Lett.* 97 (1983) 270.
- [81] I. Mayer, *Int. J. Quantum Chem.* 29 (1986) 477.
- [82] I. Mayer, *Theor. Chim. Acta* 67 (1985) 315.
- [83] V. Bonaić-Koutecký, P. Fantucci, J. Koutecký, *Phys. Rev. B* 37 (1988) 4369.
- [84] E. Janssens, H. Tanaka, S. Neukermans, R.E. Silverans, P. Lievens, *New J. Phys.* 5 (2003) 46.
- [85] R.G. Pearson, *J. Chem. Educ.* 64 (1987) 561.
- [86] R.G. Parr, P.K. Chattaraj, *J. Am. Chem. Soc.* 113 (1991) 1854.
- [87] R.G. Parr, W. Yang, *Density-functional Theory of Atoms and Molecules*, Oxford University Press, Oxford, 1989.